Iranian Journal of Science & Technology, Transaction B: Engineering, Vol. 34, No. B5, pp 567-575
Printed in The Islamic Republic of Iran, 2010

3-D DEPTH AND SUSCEPTIBILITY ESTIMATION OF MAGNETIC ANOMALIES USING LOCAL WAVENUMBER (LW) METHOD*

A. H. ANSARI** AND K. ALAMDAR

Dept. of Mining and Metallurgical Engineering, Yazd University, Yazd, I. R. of Iran
Email: h.ansari@yazduni.ac.ir

Abstract– Phase variation of potential field data can be used as an interpretation method. This idea appears in edge detection with tilt angle or phase angle. The advantages of this quantity are its independency to body magnetization direction and also its easy computations. In this paper variations of this quantity termed local wave number are used for source parameter estimation such as body depth and susceptibility, which can be used without any prior information about source geometry. This method was applied on synthetic magnetic data and on the real magnetic data of an area in the Sar-Cheshme region. Using this method, causative body depth varies from 15 to 100 meters in different locations of the studied area, which is in agreement with the existing drilling information and forward modeling.

Keywords– Depth estimation, susceptibility, potential field, tilt angle, magnetization, local wave number (LW), Sar-cheshme

1. INTRODUCTION

Magnetic data has a wide variety of applications in preliminary and detailed studies of geological structures such as magnetic sheets, contacts and faults. For example, magnetic data is used in petroleum exploration to map deposited features and faults in the basement that may control the depositional background of the sedimentary basin. In mineral exploration, the magnetic method can be used to determine the body parameters. In this case, the authentic interpretation of acquired data relies on an understanding of the structural and lithological framework, as well as the deposition pattern [1]. However, interpretation of magnetic anomalies is complicated by [2]:

1) Dipolar nature of magnetic anomalies.
2) Horizontal displacement between actual body location and characteristics points of the measured profiles. Cross–over point (corresponding to Zero value) and peak point are two common characteristic points.
3) Asymmetric shape of magnetic anomalies due to inclined vector magnetization anywhere other than magnetic poles.
4) Asymmetric shape of magnetic anomalies relevant to non-vertical structures.

Thus, potential field data interpretation, and especially magnetic data, generally requires a specialist in the potential field who is dominant in the general geology of the studied area.

Numerous methods have been designed to eliminate one or more of the mentioned complexities. Reduction to the pole [3] removes the asymmetry caused by the non-vertical magnetization direction which would have been observed in a magnetic pole. Pseudogravity converts the dipolar nature of

*Received by the editors May 11, 2009; Accepted October 13, 2009.
**Corresponding author

magnetic anomalies to monopole. In addition to the RTP technique, the horizontal displacement between the acquired anomaly and causative body location can be removed by edge detection methods. The most important methods of edge detection are zero-crossing on a second vertical derivative or by maxima on the horizontal derivative and analytic signal. Among the edge detection methods, the analytic signal has a greater application because of its independency to the body magnetization such as inclination and declination, remanent magnetization and body dip. The superposition effect due to different adjacent bodies can restrict the analytic signal application.

Another predominant way of avoiding the above interpretation complicities is to convert the total–field response into quantities that delineate the causative bodies [4]. In the past, this concept was applied on two dimensional profiles manually using a set of master curves. In this regard, the most identified methods are Peters-half slop method in depth estimation of a vertical dyke which magnetized vertically, and Half-maximum anomaly method for estimating along the z- component magnetic anomaly [1- 5]. Master curves are still used widely [6] as they do not require a computer, so they can be carried out in the field and allow the user to distinct noises from desired signals. In recent years, because of the large amount of data, the relationships between the measured anomaly and the computed anomaly due to different bodies were investigated via forward and inverse modeling [1, 2]. Automatic source parameters estimation can be accomplished either on 2-d profiles or 3-d grids. Profile techniques include the Naudy method [7], Werner deconvolution [8, 9] and 2-D Euler deconvolution [10]. Such profile techniques estimate the depth to the top of the model assuming that the strike of the structure is perpendicular to the measured line.

3-D Euler deconvolution [11], 3-D analytic signal [12] and enhanced analytic signal [13] are 3-D depth estimation methods which work on gridded data. Results from these methods are usually presented by plotting a circle having a diameter proportional to the estimated depth. Two advantages of the grid methods are that the measured line should not necessarily be perpendicular to the source strike, and the ability to make a comparison between the estimated depths in different adjacent profiles. The above 2-d and 3-D depth estimation methods are model-dependent, meaning that the reliable results are subordinate to prior information about the causative source, which in many cases because of the lack of drilling data, makes reaching this goal very difficult [14]. Salem et al present a new technique that works on either 2-D or 3-D magnetic data.

In this paper we introduced a 3-D quantitative interpretation method termed Local Wavenumber (LW) which works in the frequency domain and uses the phase variation of potential field data and its derivatives. In this method, in addition to depth estimation, a 3-D susceptibility map is produced which can be correlated with the experimental susceptibility measurements. The advantages of this method are:

1) This technique can be accomplished without any prior information about the causative source anomaly.
2) Mapping the phase variation values determines the edge of the source.
3) Results of this method are not affected by body magnetization and geomagnetic parameters, thus the presence of remanent magnetization will not disturb the outputs.
4) This method presents an estimation of source susceptibility contrast in three dimensions.

However, the intrinsic quantity of this method (local wavenumber) is a high pass nature and because the method utilizes second order derivatives of the magnetic anomaly, it is sensitive to noise. To produce more reliable results, upward continuation of the magnetic anomaly field can be applied when significant noise is present.

2. METHODOLOGY

The phase angle is defined as the angle between the vertical derivative and the absolute value of the total horizontal derivative of the potential field data, which in edge detection context is termed Tilt angle (TA). It is given by [15]:

$$T = \tan^{-1}\left(\frac{\partial f / \partial z}{\partial f / \partial h}\right) \tag{1}$$

where

$$\frac{\partial f}{\partial h} = \sqrt{\left(\frac{\partial f}{\partial x}\right)^2 + \left(\frac{\partial f}{\partial y}\right)^2} \tag{2}$$

and $\partial f / \partial x$, $\partial f / \partial y$ and $\partial f / \partial z$ are the derivatives of the magnetic field f with respect to x, y and z directions. The rate of changes of the phase angle T with respect to the x, y and z are defined as wavenumbers and are expressed as follows:

$$k_x = \frac{\partial T}{\partial x} = \frac{1}{A^2}\left(\frac{\partial f}{\partial h}\frac{\partial^2 f}{\partial x \partial z} - \frac{\partial f}{\partial z}\left(\frac{\partial f}{\partial h}\right)^{-1} \times \left(\frac{\partial f}{\partial x}\frac{\partial^2 f}{\partial x^2} + \frac{\partial f}{\partial y}\frac{\partial^2 f}{\partial y \partial x}\right)\right) \tag{3}$$

$$k_y = \frac{\partial T}{\partial y} = \frac{1}{A^2}\left(\frac{\partial f}{\partial h}\frac{\partial^2 f}{\partial y \partial z} - \frac{\partial f}{\partial z}\left(\frac{\partial f}{\partial h}\right)^{-1} \times \left(\frac{\partial f}{\partial x}\frac{\partial^2 f}{\partial x \partial y} + \frac{\partial f}{\partial y}\frac{\partial^2 f}{\partial y^2}\right)\right) \tag{4}$$

$$k_z = \frac{\partial T}{\partial z} = \frac{1}{A^2}\left(\frac{\partial f}{\partial h}\frac{\partial^2 f}{\partial z^2} - \frac{\partial f}{\partial z}\left(\frac{\partial f}{\partial h}\right)^{-1} \times \left(\frac{\partial f}{\partial x}\frac{\partial^2 f}{\partial x \partial z} + \frac{\partial f}{\partial y}\frac{\partial^2 f}{\partial y \partial z}\right)\right) \tag{5}$$

where

$$A = \sqrt{\left(\frac{\partial f}{\partial x}\right)^2 + \left(\frac{\partial f}{\partial y}\right)^2 + \left(\frac{\partial f}{\partial z}\right)^2} \tag{6}$$

is the total gradient or analytic signal of the magnetic field [16, 17, 18]. This positive quantity plays an important role in magnetic interpretation as its amplitude is independent to body magnetization direction and has been used as the edge detection and depth estimation method by many authors [19-22].

The phase angle or tilt angle has several well-known properties. It is a dimensionless quantity, its results can be evaluated by vertical or horizontal derivative, it can be differentiated with respect to the x, y and z direction as done above, and its outputs tend to equalize the amplitude [23].

Our method utilizes the tilt angle derivatives to provide a direct approach to quantify the source parameters using the definition of the Euler equation and its derivatives.

The 3-D Euler deconvolution can be defined as [11]:

$$(x - x_0)\frac{\partial f}{\partial x} + (y - y_0)\frac{\partial f}{\partial y} + (z - z_0)\frac{\partial f}{\partial z} = -Nf \tag{7}$$

where x_0, y_0 are the coordinates of the horizontal location and z_0 is the depth of the causative source, N is the structural index that describes the attenuation rate of the total magnetic field and depends on the body geometry, and z is chosen positive downward on the Cartesian coordinate system.

The above equation (Eq. (7)) is satisfied if the potential function is of the form

$$f(x-x_0, y-y_0, z-z_0) = \frac{C}{r^N} \tag{8}$$

where C is a constant independent of the coordinate origin and is associated with the physical properties of the source and

$$r = \sqrt{(x-x_0)^2 + (y-y_0)^2 + (z-z_0)^2} \tag{9}$$

Further, the horizontal and vertical derivative of various orders of potential function f will also satisfy the Euler equation. Thus, taking the derivative of the Euler deconvolution with respect to x, y and z, by following [16] we obtain

$$(x-x_0)\frac{\partial^2 f}{\partial x^2} + (y-y_0)\frac{\partial^2 f}{\partial y \partial x} + (z-z_0)\frac{\partial f}{\partial z \partial x} = -(N+1)\frac{\partial f}{\partial x} \tag{10}$$

$$(x-x_0)\frac{\partial^2 f}{\partial x \partial y} + (y-y_0)\frac{\partial^2 f}{\partial^2 y} + (z-z_0)\frac{\partial f}{\partial z \partial y} = -(N+1)\frac{\partial f}{\partial y} \tag{11}$$

$$(x-x_0)\frac{\partial^2 f}{\partial x \partial z} + (y-y_0)\frac{\partial^2 f}{\partial y \partial z} + (z-z_0)\frac{\partial f}{\partial^2 z} = -(N+1)\frac{\partial f}{\partial z} \tag{12}$$

Multiplying the Eqs. (10) and (12) by $\left(\frac{1}{A^2}\frac{\partial f}{\partial z}\frac{\partial f}{\partial x}\right)$ and $\left(\frac{1}{A^2}\left(\frac{\partial f}{\partial x}\right)^2\right)$ respectively, and subtracting the first equations from the second, we can obtain [24]:

$$\frac{(x-x_0)}{A^2}(A) + \frac{(y-y_0)}{A^2}(B) + \frac{(z-z_0)}{A^2}(C) = 0 \tag{13}$$

Where

$$A = \frac{\partial^2 f}{\partial x \partial z}\left(\frac{\partial f}{\partial x}\right)^2 - \frac{\partial^2 f}{\partial x^2}\frac{\partial f}{\partial x}\frac{\partial f}{\partial z}$$

$$B = \frac{\partial^2 f}{\partial y \partial z}\left(\frac{\partial f}{\partial x}\right)^2 - \frac{\partial^2 f}{\partial y \partial x}\frac{\partial f}{\partial x}\frac{\partial f}{\partial z}$$

$$C = \frac{\partial^2 f}{\partial z^2}\left(\frac{\partial f}{\partial x}\right)^2 - \frac{\partial^2 f}{\partial x \partial z}\frac{\partial f}{\partial x}\frac{\partial f}{\partial z}$$

Similarly multiplying equations 11 and 12 by $\left(\frac{1}{A^2}\frac{\partial f}{\partial z}\frac{\partial f}{\partial y}\right)$ and $\left(\frac{1}{A^2}\left(\frac{\partial f}{\partial y}\right)^2\right)$ respectively, and subtracting the first from the second, we obtain:

$$\frac{(x-x_0)}{A^2}(D) + \frac{(y-y_0)}{A^2}(E) + \frac{(z-z_0)}{A^2}(F) = 0 \tag{14}$$

where

$$D=\frac{\partial^2 f}{\partial x\partial z}\left(\frac{\partial f}{\partial y}\right)^2-\frac{\partial^2 f}{\partial x\partial y}\frac{\partial f}{\partial y}\frac{\partial f}{\partial z}$$

$$E=\frac{\partial^2 f}{\partial y\partial z}\left(\frac{\partial f}{\partial y}\right)^2-\frac{\partial^2 f}{\partial y^2}\frac{\partial f}{\partial y}\frac{\partial f}{\partial z}$$

$$F=\frac{\partial^2 f}{\partial z^2}\left(\frac{\partial f}{\partial y}\right)^2-\frac{\partial^2 f}{\partial y\partial z}\frac{\partial f}{\partial y}\frac{\partial f}{\partial z}$$

Adding Eqs. (13) and (14), we obtain

$$\frac{(x-x_0)}{A^2}(G)+\frac{(y-y_0)}{A^2}(H)+\frac{(z-z_0)}{A^2}(I)=0 \tag{15}$$

Where

$$G=\left(\frac{\partial f}{\partial h}\right)^2\frac{\partial^2 f}{\partial x\partial z}-\frac{\partial f}{\partial z}\left(\frac{\partial f}{\partial x}\frac{\partial^2 f}{\partial x^2}+\frac{\partial f}{\partial y}\frac{\partial^2 f}{\partial x\partial y}\right)$$

$$H=\left(\frac{\partial f}{\partial h}\right)^2\frac{\partial^2 f}{\partial y\partial z}-\frac{\partial f}{\partial z}\left(\frac{\partial f}{\partial x}\frac{\partial^2 f}{\partial x\partial y}\right)$$

$$I=\left(\frac{\partial f}{\partial h}\right)^2\frac{\partial^2 f}{\partial z^2}-\frac{\partial f}{\partial z}\left(\frac{\partial f}{\partial x}\frac{\partial^2 f}{\partial x\partial z}+\frac{\partial f}{\partial y}\frac{\partial^2 f}{\partial z\partial y}\right)$$

Dividing the last Eq. (15) by $\partial f/\partial h$ and substituting the equivalent equations defined in the tilt angle derivatives Eqs. (1), we can obtain

$$k_x x_0+k_y y_0+k_z z_0=k_x x+k_y y+k_z z \tag{16}$$

The linear Eq. (16) does not require any prior information about the source geometry and it is a very effective approach in magnetic interpretation. For solving the linear equation a progressively moving window is used. In each window there are *n* data points with known location coordinate(*x, y, z*) and wavenumbers (tilt derivatives (k_x,k_y,k_z)), so the linear equation can be written as the matrix form below:

$$Dm=d \tag{17}$$

Where *d* is the column matrix n×1 whose *i*th element is given by

$$k_{xi}x_i+k_{yi}y_i+k_{zi}z_i \tag{18}$$

D is an n×3 matrix of the tilt angle derivatives, having *i*th elements $d_{i1}=k_{xi}$, $d_{i2}=k_{yi}$, and $d_{i3}=k_{zi}$, i =1,2,3,…*n*, and three dimensional vectors $m=[x_0,y_0,z_0]$ contain the unknown source location parameters. This matrix equation can be solved using the least square method.

Estimating the susceptibility contrast, it can be achieved by the following equation [3]:

$$K=\frac{|A|}{2kFcSind} \tag{19}$$

Where $|A|$ is the amplitude of the analytic signal, k is the wavenumber, $c=1-\cos^2 i\sin^2\alpha$, i is ambient geomagnetic field inclination, α is the angle between positive *x*-axis and magnetic north and d is local dip, given by

$$d=T+2I-90 \tag{20}$$

Where $\tan I=\tan i/\cos\alpha$ and *T* is tilt angle.

3. APPLICATION TO THE SYNTHETIC MODEL

In this section, we present the application of the proposed method on the synthetic magnetic data from a vertical cylinder model. The model is located at a 500m depth and susceptibility contrast with the surrounding rocks considered o.o15 SI. The inclination and declination of the ambient magnetic field are 60^0 and 20^0 respectively. Fig. 1a, shows the magnetic response of the model. Hot and cool colors are identified with high and low intensity values respectively. Fig. 1b shows the phase variation (tilt angle) of the magnetic data in Fig. 1a, in which the minimum value determines the body boundaries. Fig. 1c shows the analytic signal map of data in Fig. 1a, in which maxima lie on the body edges. Fig. 1d presents the body depth estimation by the proposed method. The results are plotted as circles with diameters that are proportional to the estimated depth. Each circle represents 500m associated to the actual depth in producing a magnetic response. Fig. 1e shows the susceptibility contrast image of the model with respect to the surrounding rocks, and the maximum value 0.015 SI is relevant to the actual value.

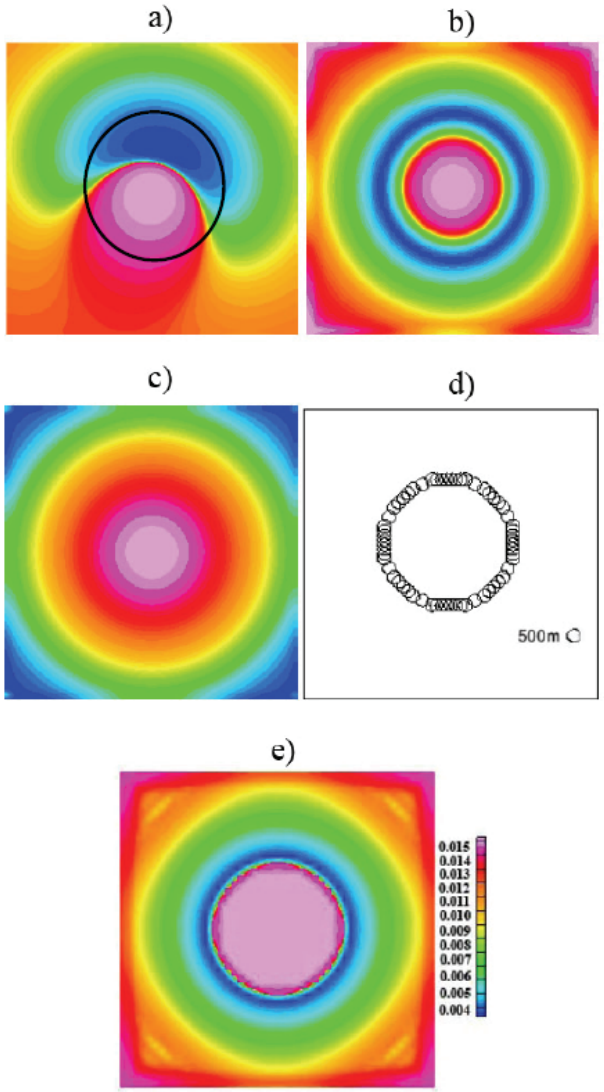

Fig. 1. Application to synthetic magnetic data: (a) Magnetic response of the vertical cylinder model located at 500m depth, inclination and declination of magnetization is 60^0 and 20^0 respectively. The black circle shows the boundary of the model. (b) Phase variation map of data in Fig. 1a. Hot colors determined high intensity, while cool colors represent the low intensity values. (c) The analytic signal amp of data in Fig. 1a. Maximum value defined the model edge. (d) Estimated depth by the proposed method plotted as a circle associated with actual body depth 500m. (e) Susceptibility contrast map of model with the surrounding area

4. APPLICATION TO THE REAL MAGNETIC DATA FROM IRAN

This case study is about an area located at $50^0\,30'$ longitude and 31^0 latitude as a part of the Rafsanjan geological quadrangle in Iran. The main magnetic potential is due to Andesite and Trachyandezite related to Eocene. The simplified geological map of the area was shown in Fig. 2. Magnetic measurement was carried out in a regular grid with 100m spacing and on 21 N-S profiles elongated 2100 meters using a GSM19T Proton magnetometer in order to determine geological structures and intrusive. Fig. 3a shows a magnetic map of the area after applying diurnal corrections. In this image, high anomalies are associated with Andesite and Trachyandesite units. The main goal of the magnetic surveying in the area is to obtain an idea about the depth of causative body for implementation of electrical prospecting. Fig. 3b presents the phase variations of data in Fig. 3a, which has a minimum that lies over the body boundaries. Fig. 3c shows the analytic signal of the magnetic data. Fig. 3d shows the susceptibility contrast, which differs from 0.031 to 0.004 in different parts of the area. In Fig. 3e the estimated depth using the presented method is plotted on the magnetic map. The circles location exposes the source boundaries and are proportional to the estimated value which ranges from 15 to 100 m and is associated with different regions and is confirmed by the available exploratory drilling information.

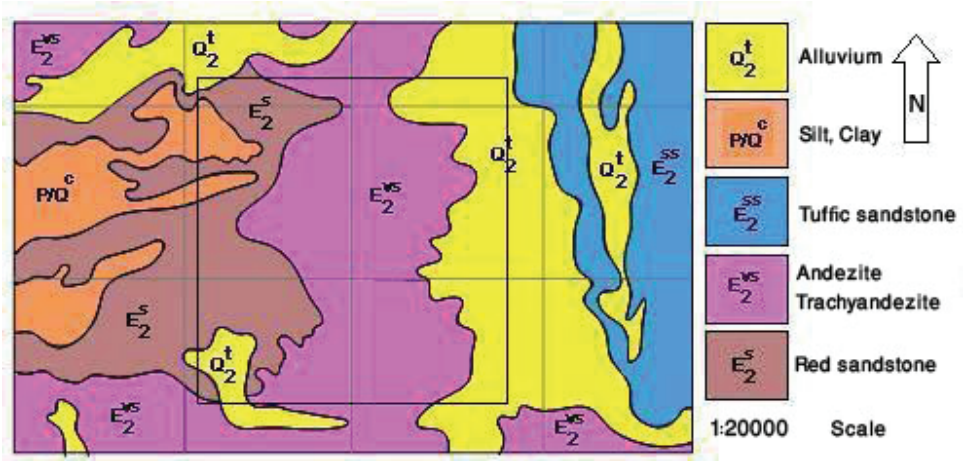

Fig. 2. Simplified geological map of the studied area (the black rectangle indicates magnetic surveying area)

5. CONCLUSION

A fast and suitable technique for the interpretation of gridded magnetic data based on derivatives of the tilt angle is presented. The method yields a linear equation to estimate the horizontal location and depth of magnetic sources without a priori information about the nature of the sources. Because the method utilizes second order derivatives of the magnetic anomaly, it is sensitive to noise in the data. To produce more reliable results, an upward continuation of the real magnetic anomaly field can be applied when significant noise is present. The presented method is independent of magnetization direction and is suitable for the interpretation of single sources or multiple magnetic sources that do not give rise to interfering anomalies. The method was tested using synthetic magnetic anomaly data over vertical cylinder model, which estimated the source parameters with adequate precision. We demonstrated the practical utility of the method by applying it to the magnetic data from an area of Iran. The results of our method show a broad correlation with the results obtained by interactive forward modeling. This method determined the causative source depth ranging from 15 to 100 m, which confirmed the field evidence.

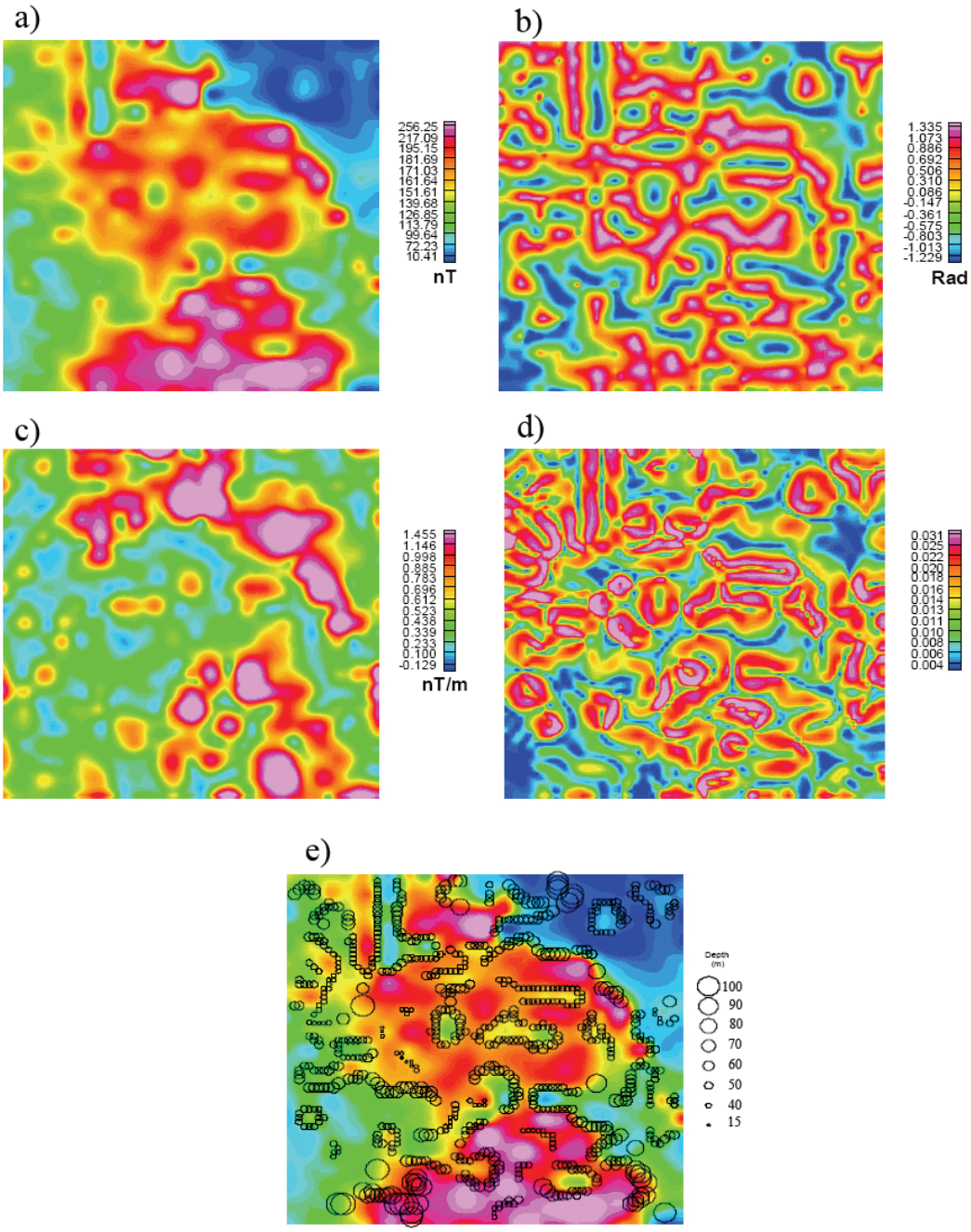

Fig. 3. Application to real magnetic data: (a) Magnetic map of the studied area. The main source of anomalies is Andesite and Trachyandesite. Data upward continued by 15m. (b) Phase angle variation of magnetic data which determines anomalies boundary. (c) The analytic signal map of data produced using (Eq. 6). (d) Susceptibility map of magnetic data differ from 0.004 to 0.031. (e) Depth estimation of causative magnetic anomalies in Fig. 3a. Depth values ranged from 15 to 100m, which is in agreement with field evidence

REFERENCES

1. Grant, F. S. & West, G. F. (1965). *Interpretation theory in applied geophysics*. McGraw-Hill Book Co.
2. Thurston, J. B. & Smith, R. S. (1997). Automatic conversion of magnetic data to depth, dip, and susceptibility contrast using the SPI method. *Geophysics*, Vol. 62, pp. 807-813.
3. Baranov, V. (1957). A new method for interpretation of aeromagnetic maps: pseudo-gravimetric anomalies. *Geophysics*, Vol. 22, pp. 359-383.

4. Thurston, J. B. & Brown, R. J. (1994). Automated source-edge location with a new variable pass-band horizontal gradient operator. *Geophysics*, Vol. 59, pp. 546-554.
5. Peters, L. J. (1949). The direct approach to magnetic interpretation and its practical application. *Geophysics*, Vol. 14, pp. 290-320.
6. Spector, A. & Lawler, T. L. (1995). Application of aeromagnetic data to mineral potential evaluation in Minnesota. *Geophysics*, Vol. 60, pp. 1704- 1714.
7. Naudy, H. (1971). Automatic determination of depth on aeromagnetic profiles. *Geophysics*, Vol. 36, pp. 712-722.
8. Hartman, R. R., Teskey, D. J. & Friedberg, J. L. (1988). A system for rapid digital aeromagnetic interpretation. *Geophysics*, Vol. 36, pp. 891-918.
9. Jian, S. (1976). An automatic method of direct interpretation of magnetic profiles. *Geophysics*, Vol. 41, pp. 531-541.
10. Thompson, D. T. (1982). EULDPH: A new technique for making computer- assisted depth estimates from magnetic data. *Geophysics*, Vol. 47, pp. 31-37.
11. Reid, A. B., Allsop, J. M., Granser, H., Millet, A. J. & Somerton, I. W. (1990). Magnetic interpretation in three dimensions using Euler deconvolution. *Geophysics*, Vol. 55, pp. 80-91.
12. Roest, W. R., Verhoef, J. & Pilkington, M. (1992). Magnetic interpretation using the 3-D analytic signal. *Geophysics*, Vol. 57, pp. 116-125.
13. Hsu, S. K., Sibuet, J. C. & Shyu, C. T. (1996). High-resolution detection of geologic boundaries from potential field anomalies: An enhanced analytic signal technique. *Geophysics*, Vol. 36, pp. 891-918.
14. Salem, A., Williams, S., Fairhead, D., Smith, R. & Ravat, D. (2008). Interpretation of magnetic data using tilt-angle derivatives. *Geophysics*, Vol. 73, No. 1, L1-L10.
15. Miller, H. G. & Singh, V. (1994). Potential field tilt- A new concept for location of potential field sources. *Journal of Applied Geophysics*, Vol. 32, pp. 213-217.
16. Nabighian, M. N. (1972). The analytic signal of two- dimensional magnetic bodies with polygonal cross-section: Its properties and use for automated anomaly interpretation. *Geophysics*, Vol. 37, pp. 507- 517.
17. Nabighian, M. N. (1984). Toward a three-dimensional automatic interpretation of potential field data via generalized Hilbert transforms: Fundamental relations. *Geophysics*, Vol. 49, pp. 780-786.
18. Atchuta Rao, D., Ram Babu, H. V. & Sanker Narayan, P. V. (1981). Interpretation of magnetic anomalies due to dikes: The complex gradient method. *Geophysics*, Vol. 46, pp. 1572-1578.
19. Haney, M., Johnston, C., Li, Y. & Nabighian, M. (2003). Envelopes of 2D and 3D magnetic data and their relationship to the analytic signal: Preliminary results. *73rd Annual International Meeting, SEG Expanded Abstracts*, pp. 596–599.
20. Hornby, P., Boschetti, F. & Horowitz., F. G. (1999). Analysis of potential field data in the wavelet domain. *Geophysical Journal International*, Vol. 137, pp. 175–196.
21. Keating, P. & Zerbo, L. (1996). An improved technique for reduction to the pole at low latitudes. *Geophysics*, Vol. 61, pp. 131–137.
22. Nabighian, M. N. & Hansen, R. O. (2001). Unification of Euler and Werner deconvolution in three dimensions via the generalized Hilbert transform. *Geophysics*, Vol. 66, pp. 1805–1810.
23. Cooper, G. R. J. & Cowan, D. R. (2006). Enhancing potential field data using filters based on the local phase. *Computer and Geosciences*, Vol. 32, pp. 1585-1591.
24. Salem, A., Ravat, D., Smith, R. & Ushijima, K. (2005). Interpretation of magnetic data using an enhanced local wavenumber (ELW) method. *Geophysics*, Vol. 70, L7-L12.